# Selection of low-energy antiprotons stopped in coordinate-sensitive calorimeter of PAMELA spectrometer

**Malakhov V V, Mayorov A G and Rodenko S A on behave of PAMELA collaboration**

National Research Nuclear University MEPhI (Moscow Engineering Physics Institute), Kashirskoe highway 31, Moscow, 115409, Russia

E-mail: sarodenko@mephi.ru, agmayorov@mephi.ru

**Abstract.** The paper presents the method of identification of low-energy antiprotons (up to ~ 1 GV), stopped in the PAMELA calorimeter, which based on the analysis of the topology of the antiprotons and secondary charged mesons tracks produced in the process of its annihilation. Applying of this method to the experimental data will the results of magnetic analysis.

## 1. Introduction

Recent experimental data on the antiproton flux in cosmic rays (CR, see [1, 2, 3]) showed a high interest in the subject, for various reasons (for example, [4-7] and references within): from the fundamental problems of astrophysics and dark matter to the applied tasks on the formation of Earth's radiation belts etc.

PAMELA is an international experiment carried out from June 2006 to February 2016 onboard the spacecraft Resurs-DK1.The results of antiproton flux obtained with the magnetic spectrometer PAMELA [8] are presented in [1] and [2]. The set of the PAMELA detectors allows to identify type of a particle with a good accuracy, performing several independent methods for cross-calibration. Thus, in both articles and the selection of antiprotons in cosmic rays was performed using the tracking system (tracker), which measured energy release and allowed to identify the sign of the charge by the particle deflection in a magnetic field. The advantage of this method is the wide energy range available for analysis (80 MeV - 350 GeV). On the other hand, at low energies (up to 400 MeV), the results may be checked and supplemented independently: by analyzing annihilation topology in a coordinate-sensitive calorimeter [8, 9], and using the information from the detectors of Time-of-Flight system [8, 10].

The sampling imaging electromagnetic calorimeter comprises 44 single-sided silicon sensor planes interleaved with 22 plates of tungsten absorber. Each plane includes 96 strips. The orientation of the strips of two consecutive layers is orthogonal and therefore provides two-dimensional spatial information.

The Time-of-Flight (ToF) systems consist of three double layers of scintillation planes, two of which are placed above the magnet and one placed between the tracker and the calorimeter. ToF is designed for providing the trigger, measuring the velocity and direction of particles arrival. The aperture of the device is determined by the geometry of the ToF.

It was shown in [10] that using the calorimeter alone isn't enough to achieve a desired level high energy protons background rejection, these protons can mimic antiprotons. For protons with a rigidity of up to 2 GV rejection was better then $10^{-5}$, but for the rigidity of ~ 3 GV it is increased by the order of magnitude. Since the expected antiprotons to protons flux ratio in CR at energies ~ 100 MeV is $0.5 \cdot 10^{-4}$:$10^{-5}$ [1] for reliable excluding of protons from the analysis, the level of rejection should be significantly better.

Therefore, compared to [10], the TOF system is proposed to include in the analysis, and we improved the identification algorithm of antiprotons in the calorimeter, by reconstruction of their tracks and adding into analyses new parameters associated with it.

## 2. Method

For creation a method of identification of antiprotons in the PAMELA experiment using the time-of-flight systems and the calorimeter isotropic flux of antiprotons and protons and π-mesons which can imitate them (born by the protons in the instrument) was simulated in the rigidity range from 0.5 to 10 GV. The simulation was performed using the PAMELA collaboration software based on Geant4 routine (model FTFP_BERT with the standard model of electromagnetic interactions) [11].

For the event selection were used the following ToF criteria: in the aperture, one hit in each plane. According to the algorithm from [10], events presumably stopped in the calorimeter were selected. It corresponds to the rigidity of protons and antiprotons ~ 0.95 GV. High energy protons and π-mesons also included in the selection.

### *2.1. Rejection high-energy protons and π-mesons*

High-energy protons and π-mesons can accidentally imitate the interaction of a particle stopped in the calorimeter and topology "star" type, characteristic of the antiproton. For their rejection, energy losses of particles in the six detectors (planes) of the ToF were used.

Figure 1 shows the energy release in the third plane versus velocity $\beta$ (as measured by the ToF) for protons and antiprotons. The energy of the stopped particles corresponds to $\beta \sim 0.7c$; this threshold is shown on the picture as vertical dashed line. This value also allows you to drop a significant part of fast particles with $\beta > 0.7c$. The lower threshold of the energy release for each detector ToF was set in the way to keep stopped protons and antiprotons (in this case, the lower threshold is 1 mip). The upper threshold was set to reject particles interacting before the plane. Due to secondary particles producing after interaction in the detectors an increasing energy releases are registered (events in a circle in figure 1).

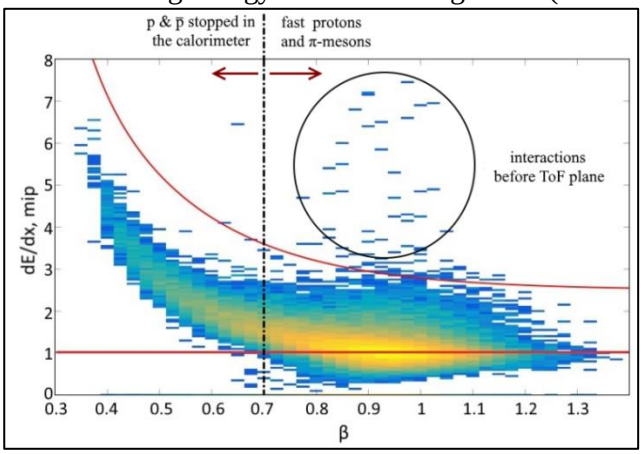


**Figure 1.** The dependence of the energy release in each of the ToF plane on the speed of protons and antiprotons

### *2.2. The reconstruction of a track of particle in the calorimeter*

The algorithm of tracks reconstruction in the calorimeter from [10] was updated and now it has a higher efficiency. Let us consider the algorithm on several illustrations of antiproton annihilation has entered vertically into the calorimeter (figure 2). On all plots of figure 2 sequence number of strips is shown along the *X*-axis and sequence number of planes in one of the projections is shown along the *Y*-axis, and the color correspond the energy release of hit strips (brighter the color corresponds to greater the energy release).

The algorithm can be represented as a series of sequential steps:

- we excluded hit strips which has no strips with signal around (figure 2a);

- we selected all strips hit in the first three planes of the calorimeter, they are shown with blue circles in figure 2b;
- we draw all tracks passing through all possible combinations of hit strips in first three planes (red lines);
- we selected the strip with the maximum energy release in the calorimeter which correspond to the point of annihilation (green circle in figure 2c);
- we chose trajectory passing closest to the point of annihilation (shown by the bold solid line); this trajectory corresponds to the real track of a particle.

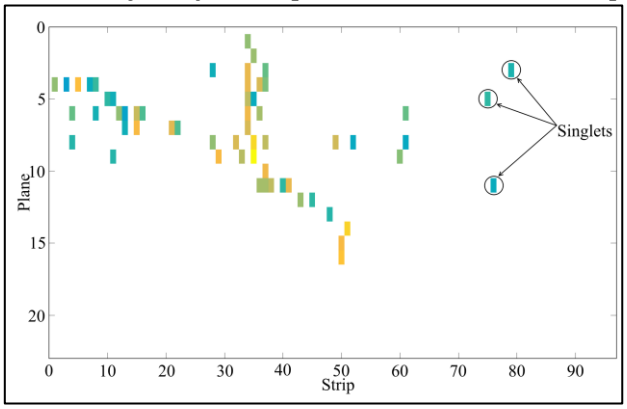


**Figure 2a.** Example antiproton annihilation in the calorimeter.

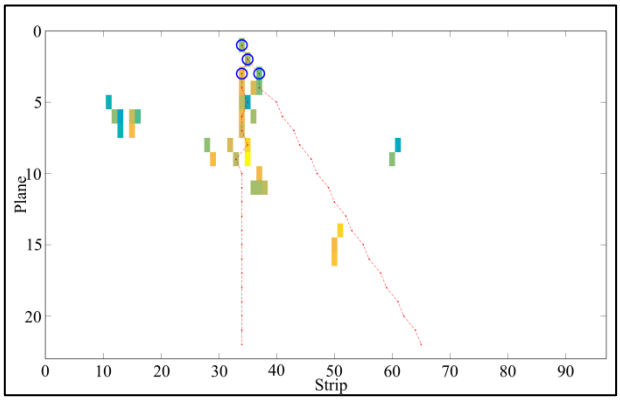


**Figure 2b.** Different combinations of the reconstructed tracks in the calorimeter.

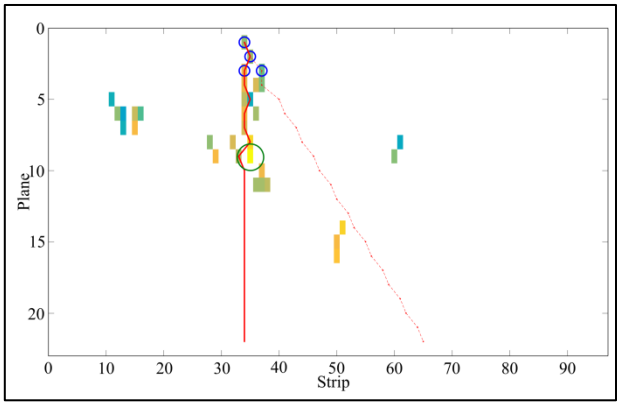


**Figure 2c.** Selecting the trajectory corresponding to the real particle.

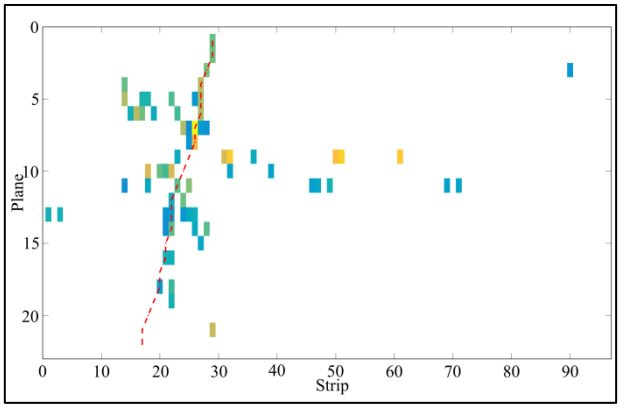


**Figure 2d.** Example antiproton annihilation in the calorimeter.

Figure 2d shows another example of the antiproton annihilation and reconstructed track.

### *2.3. Features for identification of antiprotons and their application*

In the analysis following independent features was used to separate protons and antiprotons:

- center of mass of strips with signal;
- the total number of hit strips;
- the total energy release in the calorimeter;
- ionization losses at the point of entry along the track (the first plane);
- energy release along the track (Bragg peak);
- maximum energy release along the track (expected at the point of annihilation);
- path before stopping, measured in the number of planes;
- velocity measured with ToF.

There is no possibility to describe each parameter in this article, therefore we stop just at two off them.

*2.3.1. Identification of low-energy antiprotons on the background of low-energy protons.* For antiprotons and protons separation all these parameters were used. But for illustration of the method we plot

histogram of two following parameters: the total number of hit strips and c center of mass of strips with signal (figure 3, the antiprotons are red and the protons are blue). For antiprotons the number of hit strips will be greater due to the appearance of secondary particles during annihilation.

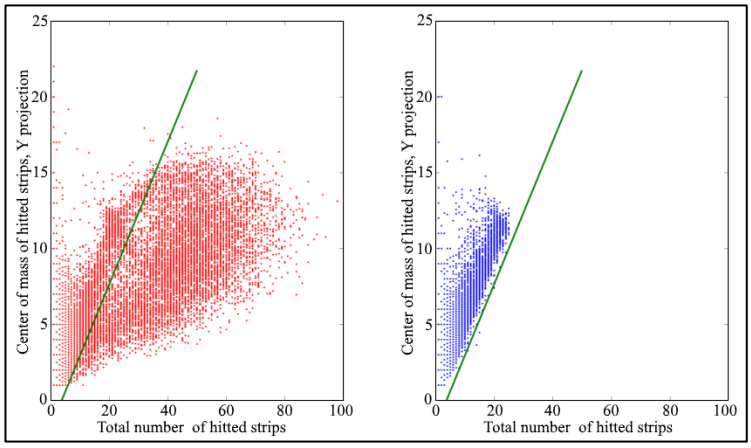


**Figure 3. The center of mass of strips with signal versus the total number of hit strips distribution.**

*2.3.2. Identification of low-energy antiprotons on the background of high-energy protons*. Protons with rigidity more then several GV do not stop in the calorimeter, but in the nuclear interactions they can produce secondary tracks in the way that whole topology will be similar to the one from antiproton annihilation. In this case protons velocity will be more than 0.9*c* and they will not stopped in the calorimeter therefor their energy release will be approximately 1 mip in each plane they pass. Distribution over the velocity and energy release at the point of entry for protons with a rigidity of more than 10 GV and antiprotons with a rigidity of up to 1 GV is plot in figure 4 (the antiprotons are red and the protons are blue). It seen that protons and antiphons regions well separated.

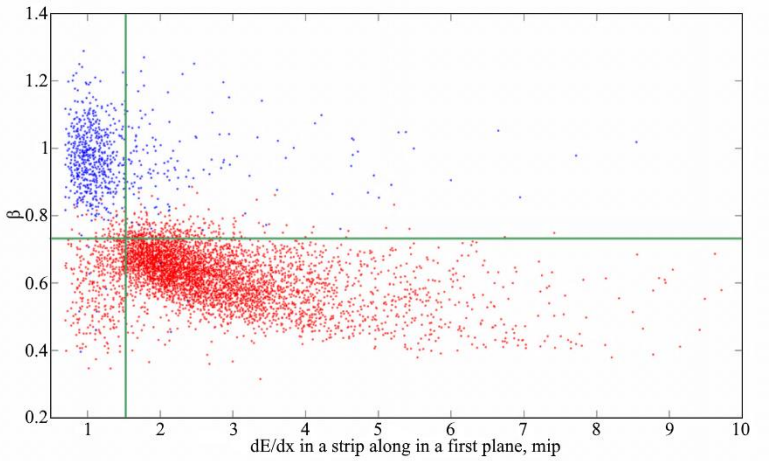


**Figure 4. Distribution over the velocity and energy release at the point of entry.**

## 3. Results and discussion

Results of method applied to independent data sample are shown in figures 5 and 6. In the figure 5 a dependence of protons and pi-mesons rejection upper limit with 95% confidence probability on particles rigidity. Obtained values allow to apply the method to experimental data. In the figure 6 a dependence of antiprotons acceptance on particles rigidity is built. Compared to tracking analysis acceptance for this method 1.8 times lower, but still enough for measurements.

In the future this technique will be applied to experimental data.

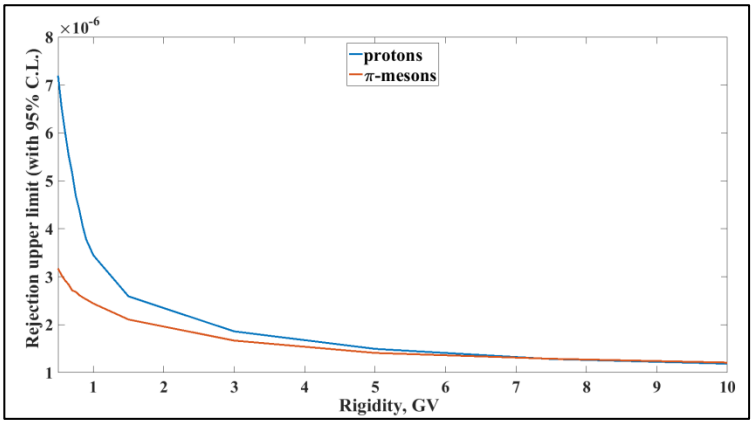


**Figure 5.** The dependence rejection of the proton and π-mesons on their rigidity.

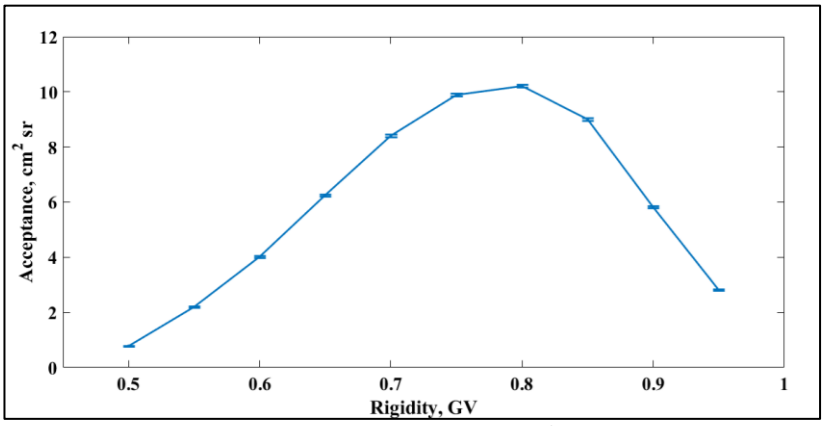


**Figure 6.** The dependence geometrical factor on rigidity.

**Acknowledgments**
This work was financially supported by RF President Grant MK-6271.2015.2 and Russian Scientific Foundation (Grant 14-12-00373).

**References**

[1] Adriani O *et al.* 2011 *Astrophys. J. Lett.* **737** 29
[2] Adriani O *et al.* 2012 *JETP* **96** 621-7
[3] Aguilar M *et al.* 2016 *Phys. Rev. Lett.* **117** 091103
[4] Bringmann T, Galea A, and Walia P 2016 *Phys. Rev.* D **93** 043529
[5] Hooper D, Linden T and Mertsch P 2015 *J. Cosmology and Astropart. Phys.* **03** 021
[6] Potgieter M *et al.* 2014 *J. Solar Phys* **289** 391-406
[7] Schwarzschild B 2011 A belt of magnetically trapped antiprotons girdles Earth *Phys. Today* **64** 10
[8] Picozza P *et al.* 2007 *Astropart. Phys.* **27** 296
[9] Boezio M *et al.* 2006 *Astropart. Phys.* **26** 111-8
[10] Menn W 2007 The ToF system of the PAMELA Experiment: In-orbit performance *Proc. of the 30th ICRC, Merida, Mexico*
[11] http://geant4.web.cern.ch/geant4/